J. Biochem. **142,** 413–419 (2007)
doi:10.1093/jb/mvm148

High-resolution Crystal Structure of β_2-Microglobulin Formed at pH 7.0†

Kentaro Iwata, Takanori Matsuura, Kazumasa Sakurai, Atsushi Nakagawa and Yuji Goto*

Institute for Protein Research, Osaka University, and CREST, Japan Science and Technology Agency, Yamadaoka 3-2, Suita, Osaka 565-0871, Japan

Received June 14, 2007; accepted July 03, 2007; published online July 23, 2007

β_2-Microglobulin (β2-m), a light chain of the major histocompatibility complex class I, forms amyloid fibrils in patients undergoing long-term haemodialysis, causing dialysis-related amyloidosis. Based on a comparison of the X-ray structure obtained at pH 5.7 and that of β2-m in the histocompatibility complex, it has been proposed that the continuous D-strand observed in the crystal structure at pH 5.7 increases the propensity of β2-m to self-associate via edge-to-edge interactions, thus initiating the formation of fibrils. To obtain further insight into the mechanism by which amyloid fibrils form, we determined the crystal structure of β2-m at pH 7.0 at a resolution of up to 1.13 Å. The crystal structure at pH 7.0 was basically the same as that at pH 5.6, suggesting that the conversion of the β-bulge in strand D into a contiguous β-strand is not unique to the crystals formed under slightly acidic conditions. In other words, although the formation of β2-m fibrils was enhanced under acidic conditions, it remains unknown if it is related to the increased propensity for the disappearance of the β-bulge in strand D. We consider that the enhanced fibrillation is more directly coupled with the decreased stability leading to the increased propensity of exposing amyloidogenic regions.

Key words: amyloid fibrils, β-bulge, dialysis-related amyloidosis, β_2-microglobulin, X-ray crystallography.

Abbreviations: β2-m, β2-microglobulin; NMR, nuclear magnetic resonance.

β_2-Microglobulin (β2-m), a light chain of the major histocompatibility complex class I (MHC-I), forms a typical immunoglobulin superfamily domain fold, where two β-sheets are linked by a disulfide bond and hydrophobic residues between them (*1*, *2*). β2-m is associated with the heavy chain through multiple hydrogen bonds on the cell surface, stabilizing the complex bound with the antigen peptide (*1*). This protein is continuously shed from the cell membrane and then fully catabolized in the kidney. Conversely, in patients undertaking long-term haemodialysis, the concentration of β2-m in plasma increases up to 60-fold (30–50 μg/ml) (*3*). Under such pathological conditions, β2-m assembles into amyloid fibrils in the joints and bones, causing a variety of arthropathies and pathological fractures, known as dialysis-related amyloidosis (*4*). As the fibrillation is a polymerization reaction, it is reasonable to consider elevated concentrations of β2-m as a critical factor leading to dialysis-related amyloidosis. However, the concentration of β2-m does not correlate with the pathology of dialysis-related amyloidosis, arguing that the elevated levels are insufficient for amyloid deposition.

The β2-m has been a target of extensive study (*5*–*11*) because of its clinical importance and suitable size for examining the relation between protein folding and the formation of amyloid fibrils. Recent studies have focused on the factors producing fibrils under neutral pH conditions where the fibrils form in patients; these include the truncation of N-terminal residues (*12*), mutations (*13*, *14*), additives such as sodium dodecyl sulfate (*15*) and interaction with Cu^{2+} ions (*12*, *16*–*19*). Nevertheless, the molecular mechanism of amyloidosis remains unclear.

To understand the mechanism by which fibrils form, it is important to reveal the structural differences between the complex and free form of β2-m. Although many structures of MHC-I complexes are deposited in the Protein Data Bank, it is only recently that the structures of the free form of β2-m have been reported (*2*, *20*–*23*). In the present study, to clarify the structure and dynamics of β2-m under neutral pH conditions, we determined the crystal structure of β2-m at pH 7.0 at a resolution of up to 1.13 Å.

MATERIALS AND METHODS

Expression and Purification of β2-m and Crystallization—Recombinant human β2-m proteins were expressed in *Escherichia coli* strain BL21(DE3) pLysS (Novagen, Madison, WI, USA) and purified as described (*23*, *24*). The protein with the expected molecular mass (±0.025%) as determined by MALDI-TOF

†The atomic coordinates for β2-m at pH 7.0 have been deposited in the Protein Data Bank (accession code: 2YXF).

*To whom correspondence should be addressed. Tel: +81-6-6879-8614, Fax: +81-6-6879-8616, E-mail: ygoto@protein.osaka-u.ac.jp

MS was shown to be ~99% pure by SDS PAGE and reverse-phase HPLC.

Crystals of monomeric β2-m were grown by the hanging-drop vapour diffusion method (*25*). For wild-type β2-m, the reservoir solution was composed of 25% (w/v) PEG 4000, 25% (v/v) glycerol, 60 mM ammonium acetate and 100 mM MOPS buffer at pH 7.0. Crystal-growth droplets were produced using 2 μl of protein solution in water (4–6 mg ml^{-1} for wild-type β2-m) and 1 μl of reservoir solution and incubating at 15°C. After 1–2 weeks, trapezium plate-like crystals appeared.

Data Collection of Intact β2-m Crystals—The intact crystals were picked up with a loop and flash-cooled at 100 K in a stream of gaseous nitrogen. X-Ray diffraction data were collected from single crystals at a wavelength of 0.650 Å with a SPring-8 (Hyogo, Japan) BL44XU beam line using an image plates X-ray detector system (Rigaku RAXIS IV^{++}). The crystal-to-detector distance was 240.0 mm. Diffraction images were indexed and integrated with MOSFLM software (*26*), and then scaled and merged with the SCALA program (CCP4) (*27*). For the intact data, molecular replacement was used for determining the structure with the MOLREP program (*28*) based on the monomeric β2-m structure (Protein Data Bank ID code 2D4F) which has been reported previously (*23*). The model refinements were performed anisotropically including hydrogen atoms by using REFMAC5 (*29*). The structure was visualized and modified using the program O (*30*). Progress was monitored by comparing the *R* factor to the free *R* factor (*31*). The geometry of the model was checked using the program PROCHECK (*32*), the Ramachandran plot showing that 99% of the residues lie in the allowed region.

RESULTS AND DISCUSSION

Crystal Structure of Monomeric β2-m at pH 7.0—The crystal structure of isolated β2-m at pH 5.7 was reported by Trinh *et al*. (*2*) (PDB ID code 1LDS). Then, the structure of a mutant, H31Y β2-m, at pH 7–8.5 (*21*, *22*) were reported (PDB ID code 1PY4). We also reported the crystal structure of wild-type (PDB ID code 2D4F) and mutant (PDB ID code 2D4D) β2-ms prepared at pH 5.7 (*23*). In our mutant W60F/W95F/L39W β2-m, the two Trp residues at 60 and 95 were replaced with Phe and a single Trp was introduced at Leu39, a position corresponding to the Trp conserved among various immunoglobulin domains. The structure of our mutant was essentially the same as that reported by Trinh *et al*. (*2*). Additionally, the NMR structure at pH 6.6 was reported (*20*) (PDB ID code 1JNJ).

The isolated β2-m and the β2-m in the MHC complex (PDB ID code 1PY4) were similar in overall structure (Fig. 1). However, careful inspection of Trinh *et al*. (*2*) revealed several differences: most importantly, the disappearance of the β-bulge in strand D of the isolated β2-m, forming one long continuous β-strand D encompassing residues 51–56 (*2*). The loss of the β-bulge results in residues 51 and 53 forming new hydrogen bonds with residues 67 and 65, respectively. This causes different orientations of the side chains of residues 50–54 [see Trinh *et al*. (*2*) for details]. Intriguingly, the NMR and crystal structures of the isolated β2-m were also different in the strand D region: only the first of two short β-strands of β2-m in the complex is retained in the β2-m monomer measured by NMR (*20–22*). Trinh *et al*. (*2*) suggested that the continuous D-strand conformation, which is rarely formed in solution, was trapped by crystallization at pH 5.7 and that, in such a conformation, β2-m's propensity to self-associate by edge-to-edge interactions is increased. However, it remains uncertain whether the D-strand is indeed involved in the formation of amyloid fibrils of β2-m, and whether the suggested critical conformation (*33*) is rarely observed in neutral pH, because of the change in the charge of His51 between pH 5.7 and pH 7.0 (*33*).

Typical crystals of intact β2-m grown at pH 7.0 reached 500 × 150 × 30 μm and diffracted with an extremely high resolution, up to 1.13 Å. A summary of the refinement statistics is given in Table 1. The intact crystal belongs to space group C2 and has the unit cell dimensions $a = 77.6$ Å, $b = 28.9$ Å, $c = 54.5$ Å and $\beta = 121.6°$, making it very similar to the structure at pH 5.7 reported by Trinh *et al*. (*2*) and also to our previously reported structures of wild-type β2-m and W60F/W95F/L39W β2-m prepared at pH 5.7 (*23*). The coordinates and structure factor amplitudes have been deposited in the Protein Data Bank (ID code 2YXF). The crystal had a very low overall B-factor, indicating that it was highly ordered (Table 1). The ribbon model and the topology diagram of the structure are shown in Fig. 1A and E, respectively.

As was the case for the acidic crystals prepared at pH 5.7 (*2*), the overall structure of β2-m at pH 7.0 was very similar to that of its MHC complex counterpart (Fig. 1). Residues involved in the β-strands include $A_{7–12}$, $B_{22–30}$, $C_{36–41}$, $C'_{43–44}$, $D_{51–56}$, $E_{62–69}$, $F_{78–83}$ and $G_{91–94}$. However, there are several differences from the structure in the MHC complex. These include slight shifts of the residues involved in β-strands, a distinct short β-strand, labelled strand C′ between strands C and D, and most importantly the disappearance of the β-bulge in strand D of the isolated β2-m forming one long continuous β-strand D encompassing residues 51–56 (Fig. 1B).

Although the structures were basically the same as those reported previously at pH 5.7 (*2*, *23*), the final electron-density map was so high that each atom density was well-separated except for disordered residues. Importantly, we could address the protonation/deprotonation of some residues. There are six Tyr residues at positions 10, 26, 63, 66, 67 and 78. Although the standard pK_a of Tyr is at basic pH (*e.g.* $pK_a = 10.1$ for amino acid Tyr), the negative 2Fo–Fc map clearly indicated the deprotonation of H_ξ of Tyr 67, suggesting a highly decreased pK_a value of Tyr 67 among the six Tyr residues (Fig. 2).

The side chain of Tyr 67 is located nearby the side chain of His51. There are four His resides at positions 13, 31, 51 and 84. It has been suggested that the pK_a value of His51 is 7.3 (*34*, *35*), higher than the others, leading to a partial positive charge at pH 7.0. This increased pK_a of His51 might be coupled with the decreased pK_a value of Tyr67.

In addition, His51 has been suggested to be the most important binding site of Cu^{2+} ions in terms of affinity and impact on the structural dynamics of β2-m (*18*, *34*, *35*). Among various factors, interaction with Cu^{2+} has

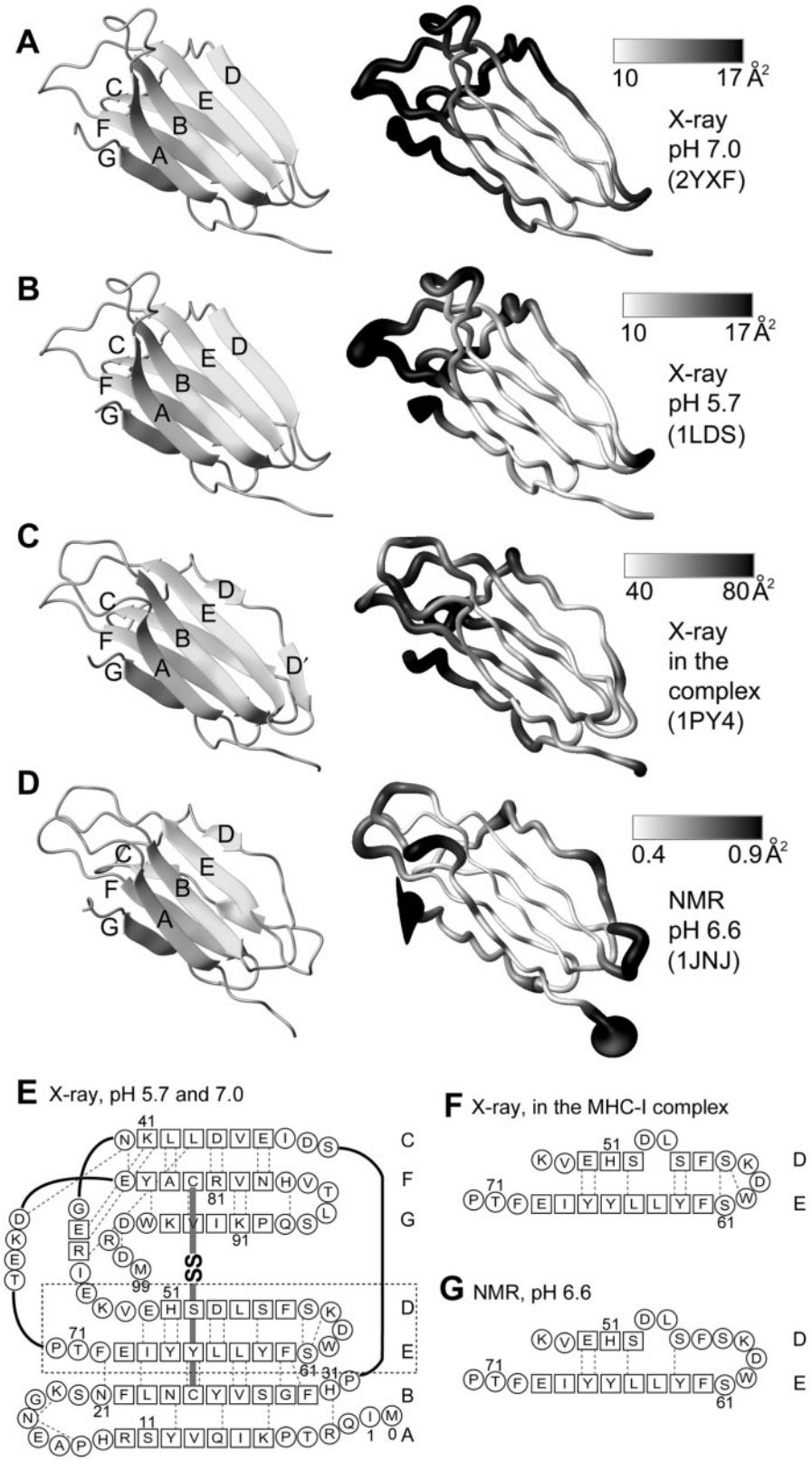

Fig. 1. **Comparison of structure of β2-m obtained under different conditions.** The crystal structure of isolated β2-m at pH 7.0 determined here (A) or at pH 5.7 by Trinh *et al*. (*2*) (B). (C) The crystal structure of β2-m in the MHC complex. (D) The NMR structure determined at pH 6.6. The ribbon models on the left were drawn by MOLMOL. The models in right indicate the B-factors (A–C) or the RMSD values of the NMR structure (D). (E–G) Topology of the crystal structure of isolated β2-m at pH 7.0 (E), that in the MHC complex (F), and that of the NMR structure (G), highlighting the inversion of strand D regions.

Table 1. **Summary of crystallographic data of wild-type β2-m.**

Summary of crystallographic data	
Crystal	Wild-type β2-m
Space group	C2
Unit cell	
a	77.64
b	28.91
c	54.40
β	121.59
Resolution	26.63–1.13 (1.19–1.13)
Number of observed reflections	146,117 (21,057)
Number of unique reflections	38,852 (5,630)
Completeness (%)	100 (100)
I/σ (I)	12.4 (4.0)
R-factor (%)	18.4
R-free (%)	20.0
Number of protein atoms	828
Number of water molecules	100
Average overall *B*-factor (Å^2)	11.14
rms deviation from ideal stereochemistry	
Bond length	0.006
Bond angle	1.45

Values in parentheses are for the highest resolution shell.

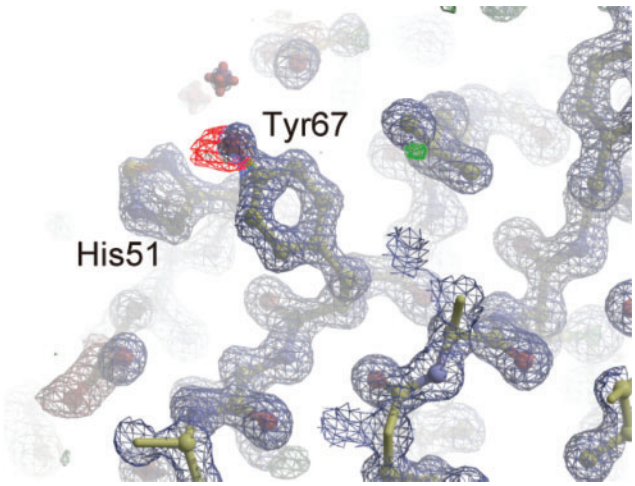

Fig. 2. **The electron-density map around Tyr67 of the crystal structure of isolated β2-m at pH 7.0.** The blue density map is a Fo–Fc map. Red and green is 2Fo–Fc map. Red and green map represent negative and positive, respectively. Although the standard pKa of Tyr occurs in far more basic conditions (*e.g.* pKa = 10.13 for the unfolded protein), the negative 2Fo–Fc map clearly indicated the deprotonation of H_ξ of Tyr 67. The figure was drawn by Coot.

been proposed to be a critical factor for triggering the formation of β2-m amyloid fibrils *in vivo*. Although the majority of Cu^{2+} is tightly bound to plasma proteins, the dialysis procedure allows interaction of β2-m with remaining free Cu^{2+} in dialysate or in cellulose membranes (*16*). *In vitro*, β2-m binds to Cu^{2+} ions specifically compared with Ca^{2+} and Zn^{2+} ions (*16*). Mutagenesis of the His residues for binding Cu^{2+} suggested that, although Cu^{2+} appears to destabilize β2-m specifically at His31 in the native state at pH 7.0, the Cu^{2+} might bind non-native forms of β2-m at His13, His51 and His84, resulting in overall destabilization (*17*). Cu^{2+} titration experiments using NMR indicated that Cu^{2+} interacts with His31, His13 (*20*) and also His51 (*18*), although the precise binding sites have not been elucidated because of the paramagnetic contribution of Cu^{2+}. In our previous study (*18*), we suggested that the binding of Cu^{2+} to His51 at pH 7.0 increases the pico- to nano-second local dynamics of β-strand D on which His51 exists, which is propagated to the core of the molecule, thus promoting the global and slow fluctuation. This may contribute to the overall destabilization of the molecule, increasing the equilibrium population of the amyloidogenic intermediate (*18*). At pH 7.0, where the side chain of Tyr67 is negatively charged, the negative charge attracts positive ions such as Cu^{2+}. This electrostatic attraction may promote the binding of Cu^{2+} to His 51. Our NMR experiments of Cu^{2+} titration (*18*) showed that upon addition of Cu^{2+}, the signal intensity for the amide proton of Tyr67 in the ^1H-^{15}N HSQC spectrum decreased more significantly at pH 7.0 than at pH 6.5. The result is consistent with the idea that the deprotonated Tyr67 side chain, located in vicinity to His51, plays a role in Cu^{2+} ion binding to His51.

We attempted to soak Cu^{2+} ions into the crystal or co-crystallize them with β2-m, but Cu^{2+} spoiled the crystals and we did not obtain enough good crystals to analyse (data not shown). This is consistent with the suggestion that the binding of Cu^{2+} to His51 is destructive to the native β2-m structure, thus promoting the formation of the amyloidogenic intermediate (*18*).

B-Factors and Structural Displacements—B-factors of the three crystallographic structures were compared (Figs 1 and 3A). On the plots, we also superimposed RMSD values of the NMR structure. The B-factor value increased in the loop regions (AB, CD, EF and GH loops) and the N- and C-terminal regions, typical of globular proteins. On the other hand, BC, FG and DE loops did not exhibit a notable increase in the B-factor. Our profile of B-factors was smooth compared with that of other structures, reflecting a high resolution. However, we did not observe a notable difference among the different crystals and the NMR structure. Then, we compared our structure with other structures, in which the regions of residues 4–11, 21–40, 46–48 and 61–94 were aligned optimally (Fig. 3B). Our structure at pH 7.0 is indistinguishable from the structure at pH 5.7 determined by Trinh *et al*. (*2*). Intriguingly, the NMR structure of β2-m at pH 6.6 is similar to the structure in the MHC complex.

Contacts between Neighbouring Molecules—Assuming that the edge-to-edge interactions initiate the formation of amyloid fibrils, it is intriguing to characterize the intermolecular interactions between monomers in the crystal lattice. Indeed, Trinh *et al*. (*2*) suggested several contacts between monomers including the D-strand in the lattice to be important to initiate fibrillation. Moreover, Rosano *et al*. (*21*) showed that the antiparallel pairing of two D2 β-strands provides two asymmetric unit-independent chains of the H31Y β2-m mutant.

A unit cell of the crystal at pH 7.0 contains four β2-m molecules, designated A–D, where the coordinates of the

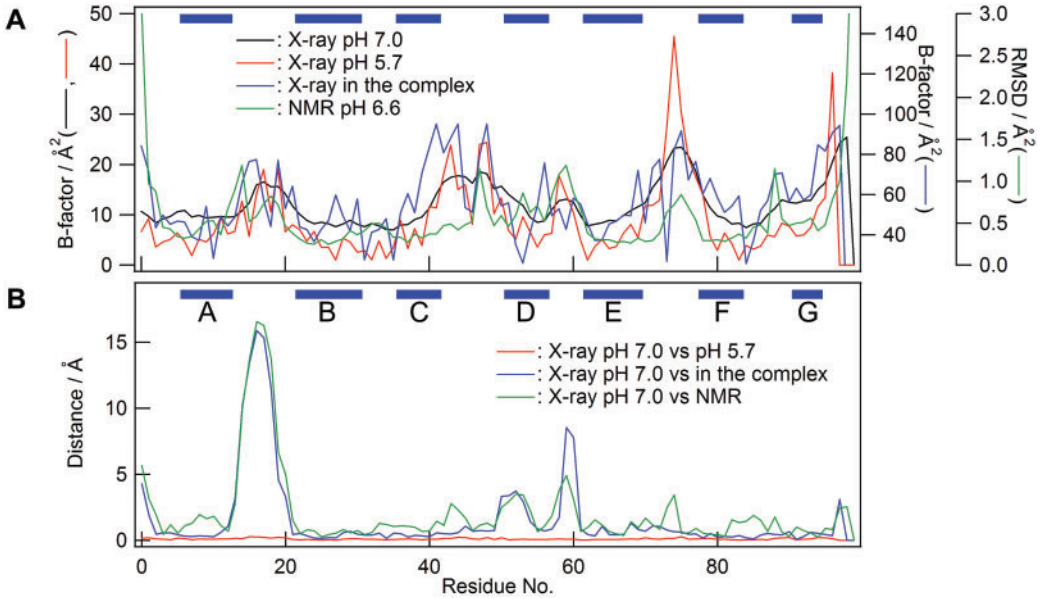

Fig. 3. **Comparison of B-factors of various structures of β2-m (A) and structural displacement between them (B).** (A) B-factors of three crystallographic structures were compared. In addition, we superimposed the RMSD values of the NMR structure. (B) The regions of residues 4–11, 21–40, 46–48 and 61–94 were aligned optimally and then displacements of Cα atoms were calculated.

four molecules are identical. Molecules A and B, and C and D assume the same symmetric unit (Fig. 4). There are a number of hydrogen bonds or salt bridges between neighbouring molecules within the lattice (Fig. 4), which are summarized in Table 2. These contacts involve the formation of a number of main-chain–main-chain hydrogen bonds between adjacent monomers in the crystal contacts (indicated by bold in Table 2). However, most of these bonds are not incorporated in an intermolecular β-sheet. Only a couple of intermolecular hydrogen bonds were observed between the extended D-strand and the neighbouring A-strand (*i.e.* one hydrogen bond between Ala15 and Leu54 and two between His13 and Phe56). In the NMR structure at pH 6.6, only the first of two short β-strands of β2-m in the complex is retained (*20–22*), suggesting that the conformation of this region fluctuates in solution. The difference between the crystal and NMR structures may be due to the crystal packing. Thus, this crystal packing does not support a process whereby β2-m fibrils form via edge-to-edge registration: although most of these intermolecular interactions are accompanied by regular crystal packing, they do not seem to extend the β-sheet leading to fibrils, as suggested by Richardson *et al*. (*36*)

CONCLUSIONS

Because monomers in solution are likely to be precursors of amyloid fibrils, it is important to characterize isolated β2-m monomers under various conditions. The present study showed that the crystallographic structure of β2-m monomers at pH 7.0 is essentially the same as that at pH 5.6. Thus, the conversion of the β-bulge in strand D into a contiguous β-strand is not unique to slightly acidic conditions (*2*). In other words, although the formation of

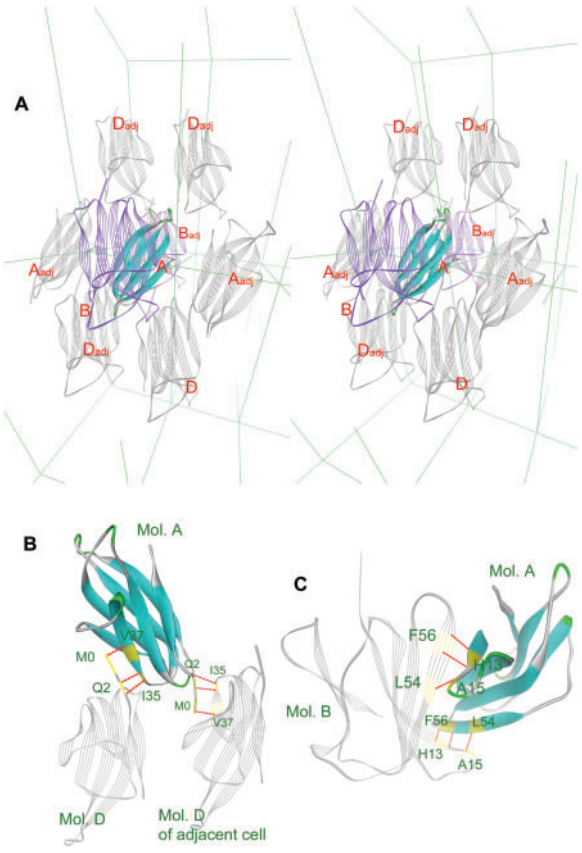

Fig. 4. **The intermolecular contacts in the crystal structure of β2-m at pH 7.0.** (A) Molecular packing in the crystals. (B, C) Intermolecular main-chain–main-chain hydrogen bonds between adjacent monomers as indicated in Table 2.

Table 2. **List of intermolecular hydrogen bonds and salt bridges in the lattice of the β2-m crystal.**

Mol.	Res.	Atom	Position		Mol.	Res.	Atom	Position
Hydrogen bonds								
A	R12	NH_2	βA	-	B	Y26	OH	βB
A	**H13**	**N**	**AB lo**	**-**	**B**	**F56**	**O**	**βD**
A	**A15**	**N**	**AB lo**	**-**	**B**	**L54**	**O**	**βD**
A	**F56**	**N**	**βD**	**-**	**B**	**H13**	**O**	**AB lo**
A	K58	Nζ	DE lo	-	B	D98	O	C term
A	S33	O	BC lo	-	D	Q2	Nε2	N term
A	S33	Oγ	BC lo	-	D	T4	Oδ1	N term
A	S33	Oγ	BC lo	-	D	T86	O	FG lo
A	D34	Oδ1	BC lo	-	D	T4	Oδ1	N term
A	D34	Oδ2	BC lo	-	D	T4	N	N term
A	**I35**	**N**	**BC lo**	**-**	**D**	**Q2**	**O**	**N term**
A	**I35**	**O**	**BC lo**	**-**	**D**	**Q2**	**N**	**N term**
A	V37	N	βC	-	D	M0	O,Sδ	N term
A	**V37**	**O**	**βC**	**-**	**D**	**M0**	**N**	**N term**
A	D38	Oδ1	βC	-	D	M0	N	N term
A	D59	O	DE lo	-	D	S88	Oδ	FG lo
A	Y66	OH	βE	-	D	M0	N	N term
Salt bridges								
A	K58	Nζ	DE lo	-	B	D98	O,Oδ1	C term
A	D38	Oδ1	βC	-	D	M0	N	N term

β2-m fibrils was evidently enhanced under slightly acidic conditions (*11*, *37*), it remains unknown if it is related to the increased propensity of the disappearance of the β-bulge in strand D. Moreover, we did not see any significant symptoms of oligomerization through the edge-to-edge association of strands in the lattice. Although dimers associated through facing D-strands were observed in the H31Y β2-m (*21*, *22*), to extend a linear amyloid polymer, at least one entry and one exit point on each monomeric unit is required. Furthermore, the NMR study at pH 6.6 suggests partial disordering of the D-strand, a conformational change directing opposite to the edge-to-edge association (*20*, *21*, *35*). Thus, the role of edge-to-edge associations in forming amyloid fibrils of β2-m remains unclear. Instead, we consider that the enhanced fibrillation of β2-m under slightly acidic conditions is more directly coupled with the decreased stability leading to the increased propensity of exposing amyloidogenic regions (*12*, *35*, *37*).

REFERENCES

1. Bjorkman, P.J., Saper, M.A., Samraoui, B., Bennett, W.S., Strominger, J.L., and Wiley, D.C. (1987) Structure of the human class I histocompatibility antigen, HLA-A2. *Nature* **329**, 506–512
2. Trinh, C.H., Smith, D.P., Kalverda, A.P., Phillips, S.E., and Radford, S.E. (2002) Crystal structure of monomeric human β2-microglobulin reveals clues to its amyloidogenic properties. *Proc. Natl Acad. Sci. USA* **99**, 9771–9776
3. Floege, J. and Ehlerding, G. (1996) β2-Microglobulin-associated amyloidosis. *Nephron* **72**, 9–26
4. Gejyo, F., Yamada, T., Odani, S., Nakagawa, Y., Arakawa, M., Kunitomo, T., Kataoka, H., Suzuki, M., Hirasawa, Y., Shirahama, T., Cohen, A.S., and Schmid, K. (1985) A new form of amyloid protein associated with chronic hemodialysis was identified as β2-microglobulin. *Biochem. Biophys. Res. Commun.* **129**, 701–706
5. Naiki, H., Hashimoto, N., Suzuki, S., Kimura, H., Nakakuki, K., and Gejyo, F. (1997) Establishment of a kinetic model of dialysis-related amyloid fibril extension in vitro. *Amyloid* **4**, 223–232
6. Kozhukh, G.V., Hagihara, Y., Kawakami, T., Hasegawa, K., Naiki, H., and Goto, Y. (2002) Investigation of a peptide responsible for amyloid fibril formation of β2-microglobulin by Achromobacter protease I. *J. Biol. Chem.* **277**, 1310–1315
7. Katou, H., Kanno, T., Hoshino, M., Hagihara, Y., Tanaka, H., Kawai, T., Hasegawa, K., Naiki, H., and Goto, Y. (2002) The role of disulfide bond in the amyloidogenic state of β2-microglobulin studied by heteronuclear NMR. *Protein Sci.* **11**, 2218–2229
8. Hoshino, M., Katou, H., Hagihara, Y., Hasegawa, K., Naiki, H., and Goto, Y. (2002) Mapping the core of the β2-microglobulin amyloid fibril by H/D exchange. *Nat. Struct. Biol.* **9**, 332–336
9. Ban, T., Yamaguchi, K., and Goto, Y. (2006) Direct observation of amyloid fibril growth, propagation, and adaptation. *Acc. Chem. Res.* **39**, 663–670
10. Jahn, T.R., Parker, M.J., Homans, S.W., and Radford, S.E. (2006) Amyloid formation under physiological conditions proceeds via a native-like folding intermediate. *Nat. Struct. Mol. Biol.* **13**, 195–201
11. McParland, V.J., Kalverda, A.P., Homans, S.W., and Radford, S.E. (2002) Structural properties of an amyloid precursor of β2-microglobulin. *Nat. Struct. Biol.* **9**, 326–331
12. Esposito, G., Michelutti, R., Verdone, G., Viglino, P., Hernandez, H., Robinson, C.V., Amoresano, A., Dal Piaz, F., Monti, M., Pucci, P., Mangione, P., Stoppini, M., Merlini, G., Ferri, G., and Bellotti, V. (2000) Removal of the N-terminal hexapeptide from human β2-microglobulin facilitates protein aggregation and fibril formation. *Protein Sci.* **9**, 831–845
13. Kad, N.M., Thomson, N.H., Smith, D.P., Smith, D.A., and Radford, S.E. (2001) β2-Microglobulin and its deamidated variant, N17D form amyloid fibrils with a range of morphologies in vitro. *J. Mol. Biol.* **313**, 559–571
14. Jones, S., Smith, D.P., and Radford, S.E. (2003) Role of the N and C-terminal strands of β2-microglobulin in amyloid formation at neutral pH. *J. Mol. Biol.* **330**, 935–941
15. Yamamoto, S., Hasegawa, K., Yamaguchi, I., Tsutsumi, S., Kardos, J., Goto, Y., Gejyo, F., and Naiki, H. (2004) Low concentrations of sodium dodecyl sulfate induce the extension of β2-microglobulin-related amyloid fibrils at a neutral pH. *Biochemistry* **43**, 11075–11082
16. Morgan, C.J., Gelfand, M., Atreya, C., and Miranker, A.D. (2001) Kidney dialysis-associated amyloidosis: a molecular role for copper in fiber formation. *J. Mol. Biol.* **309**, 339–345
17. Eakin, C.M., Knight, J.D., Morgan, C.J., Gelfand, M.A., and Miranker, A.D. (2002) Formation of a copper specific binding site in non-native states of β2-microglobulin. *Biochemistry* **41**, 10646–10656
18. Villanueva, J., Hoshino, M., Katou, H., Kardos, J., Hasegawa, K., Naiki, H., and Goto, Y. (2004) Increase in the conformational flexibility of β2-microglobulin upon copper binding: a possible role for copper in dialysis-related amyloidosis. *Protein Sci.* **13**, 797–809
19. Eakin, C.M., Berman, A.J., and Miranker, A.D. (2006) A native to amyloidogenic transition regulated by a backbone trigger. *Nat. Struct. Mol. Biol.* **13**, 202–208
20. Verdone, G., Corazza, A., Viglino, P., Pettirossi, F., Giorgetti, S., Mangione, P., Andreola, A., Stoppini, M., Bellotti, V., and Esposito, G. (2002) The solution structure of human β2-microglobulin reveals the prodromes of its amyloid transition. *Protein Sci.* **11**, 487–499
21. Rosano, C., Zuccotti, S., Mangione, P., Giorgetti, S., Bellotti, V., Pettirossi, F., Corazza, A., Viglino, P., Esposito, G., and Bolognesi, M. (2004) β2-Microglobulin

H31Y variant 3D structure highlights the protein natural propensity towards intermolecular aggregation. *J. Mol. Biol.* **335**, 1051–1064
22. Rosano, C., Zuccotti, S., and Bolognesi, M. (2005) The three-dimensional structure of β2 microglobulin: results from X-ray crystallography. *Biochim. Biophys. Acta* **1753**, 85–91
23. Kihara, M., Chatani, E., Iwata, K., Yamamoto, K., Matsuura, T., Nakagawa, A., Naiki, H., and Goto, Y. (2006) Conformation of amyloid fibrils of β2-microglobulin probed by tryptophan mutagenesis. *J. Biol. Chem.* **281**, 31061–31069
24. Chiba, T., Hagihara, Y., Higurashi, T., Hasegawa, K., Naiki, H., and Goto, Y. (2003) Amyloid fibril formation in the context of full-length protein: effects of proline mutations on the amyloid fibril formation of β2-microglobulin. *J. Biol. Chem.* **278**, 47016–47024
25. McPherson, A. (1992) Two approaches to the rapid screening of crystallization conditions. *J. Cryst. Growth* **122**, 161–167
26. Leslie, A.G.W. (1992) *Joint CCP4 and ESF-EACBM Newsletter on Protein Crystallography* Vol. 26, Science and Engineering Research Council, Daresbury Lab, Warrington, UK
27. CCP4 Collaborative Computational Project, Number 4.(1994) *Acta Crystallogr. Sect. D* **50**, 760–763
28. Vagin, A. and Teplyakov, A. (1997) MOLREP: an automated program for molecular replacement. *J. Appl. Cryst.* **30**, 1022–1025
29. Murshudov, G.N., Vagin, A.A., and Dodson, E.J. (1997) Refinement of macromolecular structures by the maximum-likelihood method. *Acta Crystallogr. D Biol. Crystallogr.* **D53**, 240–255
30. Jones, T.A., Zou, J.Y., Cowan, S.W., and Kjeldgaard, M. (1991) Improved methods for building protein models in electron density maps and the location of errors in these models. *Acta Crystallogr. Sec. A* **47**, 110–119
31. Brunger, A.T. (1992) Free R value: a novel statistical quantity for assessing the accuracy of crystal structures. *Nature* **355**, 472–475
32. Laskowski, R.A., Rullmannn, J.A., MacArthur, M.W., Kaptein, R., and Thornton, J.M. (1996) AQUA and PROCHECK-NMR: programs for checking the quality of protein structures solved by NMR. *J. Biomol. NMR* **8**, 477–486
33. Park, S. and Saven, J.G. (2006) Simulation of pH-dependent edge strand rearrangement in human β2 microglobulin. *Protein Sci.* **15**, 200–207
34. Corazza, A., Pettirossi, F., Viglino, P., Verdone, G., Garcia, J., Dumy, P., Giorgetti, S., Mangione, P., Raimondi, S., Stoppini, M., Bellotti, V., and Esposito, G. (2004) Properties of some variants of human β2-microglobulin and amyloidogenesis. *J. Biol. Chem.* **279**, 9176–9189
35. Esposito, G., Corazza, A., Viglino, P., Verdone, G., Pettirossi, F., Fogolari, F., Makek, A., Giorgetti, S., Mangione, P., Stoppini, M., and Bellotti, V. (2005) Solution structure of β2-microglobulin and insights into fibrillogenesis. *Biochim. Biophys. Acta* **1753**, 76–84
36. Richardson, J.S. and Richardson, D.C. (2002) Natural β-sheet proteins use negative design to avoid edge-to-edge aggregation. *Proc. Natl Acad. Sci. USA* **99**, 2754–2759
37. Ohhashi, Y., Hasegawa, K., Naiki, H., and Goto, Y. (2004) Optimum amyloid fibril formation of a peptide fragment suggests the amyloidogenic preference of β2-microglobulin under physiological conditions. *J. Biol. Chem.* **279**, 10814–10821